

1 **Raman spectroscopic techniques to detect ovarian cancer**
2 **biomarkers in blood plasma**

3
4 Maria Paraskevaïdi^{a,1}, Katherine M. Ashton^b, Helen F. Stringfellow^b, Nicholas Wood^c,
5 Patrick Keating^c, Anthony Rowbottom^d, Pierre L. Martin-Hirsch^c and Francis L. Martin^{a,1}

6 *^aSchool of Pharmacy and Biomedical Sciences, University of Central Lancashire, Preston PR1*
7 *2HE, UK*

8 *^bPathology Department, Lancashire Teaching Hospitals NHS Foundation Trust, Preston PR2*
9 *9HT, UK*

10 *^cDepartment of Obstetrics and Gynaecology, Lancashire Teaching Hospitals NHS Foundation*
11 *Trust, Preston PR2 9HT, UK*

12 *^dImmunology Laboratory, Pathology Department, Lancashire Teaching Hospitals NHS*
13 *Foundation Trust, Preston PR2 9HT, UK*

14
15
16
17
18
19
20
21
22
23 ¹To whom correspondence should be addressed. Email: mparaskevaïdi@uclan.ac.uk or
24 flmartin@uclan.ac.uk Tel: +44 (0) 1772 89 6482

25 Abstract

26 Robust diagnosis of ovarian cancer is crucial to improve patient outcomes. The lack of a single
27 and accurate diagnostic approach necessitates the advent of novel methods in the field. In the
28 present study, two spectroscopic techniques, Raman and surface-enhanced Raman
29 spectroscopy (SERS) using silver nanoparticles, have been employed to identify signatures
30 linked to cancer in blood. Blood plasma samples were collected from 27 patients with ovarian
31 cancer and 28 with benign gynecological conditions, the majority of which had a prolapse.
32 Early ovarian cancer cases were also included in the cohort ($n=17$). The derived information
33 was processed to account for differences between cancerous and healthy individuals and a
34 support vector machine (SVM) algorithm was applied for classification. A subgroup analysis
35 using CA-125 levels was also conducted to rule out that the observed segregation was due to
36 CA-125 differences between patients and controls. Both techniques provided satisfactory
37 diagnostic accuracy for the detection of ovarian cancer, with spontaneous Raman achieving
38 94% sensitivity and 96% specificity and SERS 87% sensitivity and 89% specificity. For early
39 ovarian cancer, Raman achieved sensitivity and specificity of 93% and 97%, respectively,
40 while SERS had 80% sensitivity and 94% specificity. Five spectral biomarkers were detected
41 by both techniques and could be utilised as a panel of markers indicating carcinogenesis. CA-
42 125 levels did not seem to undermine the high classification accuracies. This minimally
43 invasive test may provide an alternative diagnostic and screening tool for ovarian cancer that
44 is superior to other established blood-based biomarkers.

45

46

47

48 **Keywords:** Ovarian cancer; diagnostics; biospectroscopy; Raman; SERS

49 Introduction

50 Ovarian cancer is frequently discovered at a late stage due to non-specific
51 symptomatology. More than 70% of ovarian cancer patients are diagnosed at an advanced state
52 (stage IV) when the five-year survival rate is 25% [1]. Ideally, disease should be diagnosed
53 promptly and at an early stage (stage I), when cancer is completely confined to the ovaries, as
54 stages II, III and IV are considered advanced with cancer being spread outside the ovaries into
55 the pelvis (*e.g.*, fallopian tubes, bladder or rectum), abdominal cavity (*e.g.*, lining of the
56 abdomen or lymph nodes) and other distinct organs (*e.g.*, lungs), respectively [2]. As a
57 consequence, the five-year survival rate of stage II patients is increased to 70%, while for stage
58 I patients it is further increased to 90% [1, 3].

59 Screening or diagnostic tests for ovarian cancer comprise of cancer antigen CA-125
60 alone, ultrasound imaging of the ovaries or a combination. These tests have different screening
61 utility depending on whether they are applied in low or high risk populations. However neither,
62 even in combination, have robust levels of diagnostic accuracy [4, 5]. A variety of blood tests
63 have also been developed with CA 19-9, human epididymis protein 4 (HE4), apolipoprotein
64 A1 (ApoA1), insulin growth factor II (IGF-II) and transferrin being some of them [6-9].
65 However, most of these individual biomarker tests yield unacceptable diagnostic accuracies
66 which render them unsuitable for clinical use. Recent strategies attempt to combine a number
67 of these tests to achieve superior performance.

68 Raman spectroscopy has been used extensively in cancer diagnostics utilising a variety
69 of samples (*e.g.*, cells, tissues or biological fluids). Other diagnostic techniques, such as optical
70 coherence tomography, fluorescence microscopy or nonlinear microscopy could also be used
71 for diagnostic purposes, however Raman spectroscopy has been shown in many cases to
72 provide better results [10]. Cervical, skin, breast, oral and brain cancers, as well as other
73 diseases, are some of the wide applications of Raman, facilitating disease detection/monitoring

74 or even intraoperative assessment of surgical margins [11-19]. Moreover, previous
75 spectroscopic studies have successfully investigated ovarian tissue post-surgery and showed
76 significant differences between normal and malignant cases [20-22]. However, the use of
77 biological fluids, such as blood samples, are numerous: minimally-invasive collection, easier
78 sample preparation and collection of serial samples from the same participants, just to name a
79 few [23, 24]. Raman spectroscopy investigates the phenomenon of inelastic light scattering that
80 is caused after the interaction of light with matter. The sample's electrons first get excited to a
81 virtual state and then fall back to their original energy level either by losing or by gaining
82 energy. The generated shift in energy is characteristic for specific biomolecules such as
83 proteins, lipids and nucleic acids, providing thus invaluable information for a biological
84 sample.

85 Raman scattering is inherently weak and, therefore, enhancement techniques have been
86 developed to increase the derived signal [25]. Surface-enhanced Raman spectroscopy (SERS)
87 is one of the commonly applied methods which utilises rough metallic surfaces or
88 nanostructures (*e.g.*, silver or gold nanoparticles) to increase the Raman signal by 10^3 - 10^{10}
89 times. SERS exploits the great electromagnetic field enhancement that is caused by oscillations
90 of surface electrons, called surface plasmons [26]. This allows detection of molecules at low
91 concentration and can partly account for fluorescence that may distort the spectra [15, 27].

92 The main objective of this study was to use blood spectroscopy in order to assess the
93 diagnostic accuracy for ovarian cancer in women with both early- and late-stage cancer, which
94 has not been previously attempted. Extraction of differential spectral biomarkers was also
95 performed and tentative assignments were made for the development of a panel of diagnostic
96 markers. An important confounding factor, which has not been taken into account in previous
97 spectroscopic studies, and could lead to falsified classification between cancer and healthy
98 controls was the CA-125 level; therefore its effect on the spectral results has been now

99 calculated in a separate subgroup analysis. To the best of our knowledge this is also the first
100 study employing both Raman and SERS to investigate the effect of the enhanced approach in
101 the diagnostic accuracy – does increased signal necessarily imply improved diagnostic
102 accuracy as well?

103 **Materials and Methods**

104 **Population**

105 This study included 27 women with ovarian cancer (17/27 stage I) and 28 women with
106 benign gynecological conditions or a prolapse. All specimens were collected with ethical
107 approval obtained at Royal Preston Hospital UK (16/EE/0010). Mean-age was 68 years for the
108 cancer group and 56 years for the non-cancer group. More information about the cohort
109 characteristics can be found in Table 1; more detailed information about each participant is
110 given in Table S1 [see Supplementary Information (SI)]. Age difference between the different
111 groups was also taken into account to demonstrate whether it affected the spectral results, and
112 therefore the diagnostic accuracy (see SI Fig. S1). Women who were on Tamoxifen have been
113 excluded.

114 **CA-125 measurement**

115 CA-125 levels were determined in blood serum samples for both the ovarian cancer patients
116 and healthy individuals. This test, is a two-site sandwich immunoassay using
117 electrochemiluminescence (ECL) technology which uses monoclonal antibodies (Elecsys CA
118 125 II, Roche Diagnostics GmbH). The system (Roche Cobas 8000) automatically dispenses
119 20 µl of sample into a cuvette and then dispenses a biotinylated CA125-specific antibody and
120 a CA125-specific antibody labelled with ruthenium complex react to form a sandwich complex.
121 Streptavidin microparticles are then added and the complex becomes bound to the solid phase
122 *via* the interaction of biotin and streptavidin. The reaction mixture is aspirated in to the reaction

123 cell where the microparticles are magnetically captured onto the surface of the electrode.
124 Unbound substances are then removed with Procell solution. Application of a voltage to the
125 electrode induces the chemiluminescent emission, which is measured by the photomultiplier;
126 the results are then determined via a calibration curve. A direct relationship exists between the
127 amount of CA-125 in sample and the amount of photons detected by the system. The reference
128 range of CA-125 is 0-35 units/ml (0-35 kU/L), with values >35 kU/L indicating an increased
129 probability for residual or recurrent ovarian cancer in patients treated for primary epithelial
130 ovarian cancer.

131 **Blood plasma preparation for spontaneous Raman and SERS analysis**

132 Whole blood was collected into EDTA tubes, centrifuged at 2000 rpm for 10 min to
133 remove the cells (erythrocytes, white blood cells and platelets) from plasma. The supernatant
134 was then collected and stored at -80°C and thawed at room temperature prior to spectroscopic
135 interrogation. After the samples were thawed, 50 µL were deposited directly on aluminium foil
136 slides and left to air-dry. In order to employ SERS as an enhancement method, silver
137 nanoparticles (AgNPs), with a diameter of 100 nm, were used (nanoComposix, Inc., San
138 Diego). The stock solution (mass concentration: 1.02 mg/ml) was diluted in phosphate buffered
139 saline (PBS); 1 µl AgNPs was diluted in 100 µl PBS. Fifty µl of the diluted solution were mixed
140 with 50 µl of the biological fluid and the resulting mixture (100 µl) was then deposited on
141 aluminium foil slides and was again left to air-dry at room temperature before Raman spectra
142 were acquired.

143 **Spectral acquisition**

144 The experimental settings were kept the same for both Raman and SERS analysis.
145 Spectra were collected with an InVia Renishaw Raman spectrometer coupled with a charge-
146 coupled device (CCD) detector and a Leica microscope. A 785 nm laser was used with a 1200
147 l/mm grating and the system was calibrated to 520.5 cm⁻¹ by using a silicon source before every

148 run. Seven point spectra were acquired per sample using a 50× objective, 10 second exposure
149 time, 5% laser power and 2 accumulations in the spectral range of 2000-400 cm⁻¹ to achieve
150 optimum spectral quality.

151 **Spectral pre-processing and classification**

152 Spectra were evaluated during collection and any cosmic rays were removed by using
153 the Renishaw WiRe software. An in-house developed IRootLab toolbox
154 (<http://trevisanj.github.io/irootlab/>) was then implemented within MATLAB environment
155 (MathWorks, Natick, USA) for further pre-processing and classification of the data. An initial
156 pre-processing phase is required to deal with any background noise or non-biological
157 variability associated with spectral acquisition or instrumentation. Herein, all spectra were
158 firstly truncated to the biological region (1800-500 cm⁻¹), wavelet denoised, polynomial
159 baseline corrected and vector normalized. All of these steps are standard in the Raman analysis
160 of biological samples in order to generate noise-free spectra with conventional appearance [27].
161 Difference-between-mean (DBM) spectra was also performed to extract potential biomarkers
162 by subtracting the mean spectra of two classes (*i.e.*, ovarian cancer patients and controls); a
163 peak detection algorithm was implemented to identify the ten most segregating peaks.

164 Support vector machine (SVM) is a supervised machine-learning technique for creating
165 a classification function from training data. Some of the criteria for the choice of classifier
166 include the achieved diagnostic accuracy, as well as training and computational time [28]. For
167 SVM implementation, the already pre-processed dataset was further normalized (to the [0, 1]
168 range) in order to put all the variables on the same scale. We used the Gaussian kernel SVM,
169 which implies that there are two parameters to be tuned to the value that gives best
170 classification: *c* and *gamma* [29]. The optimal tuning parameters were found using grid search
171 (5-fold cross-validation) and then used to calculate the sensitivity and specificity for the
172 different comparisons [29, 30]. Sensitivity is defined as the probability of a test being positive

173 when the disease is present, while specificity is defined as the probability that a test will be
174 negative at the absence of disease; they were calculated by the following equations:

$$175 \text{ Sensitivity}(\%) = \frac{TP}{TP+FN} \times 100 \quad (1)$$

$$176 \text{ Specificity}(\%) = \frac{TN}{TN+FP} \times 100 \quad (2)$$

177 where TP is defined as true positive; FN as false negative; TN as true negative; and FP as false
178 positive.

179 **Statistical analysis**

180 The common peaks that were found to differentiate the classes in both Raman and
181 SERS, after the implementation of the DBM algorithm, were further analyzed in GraphPad
182 Prism 7.0 (GraphPad Software Inc., La Jolla, CA, USA). A student's t-test (non-parametric,
183 two-tailed, 95% confidence interval (CI)) was performed to account for statistical significance
184 with a *P*-value of 0.05 or less being considered significant. Statistical analysis was carried out
185 on averaged spectra in order to account for differences between individuals and not spectra.

186 **Availability of data**

187 All data (raw and pre-processed spectra) along with appropriate code identifiers will be
188 uploaded onto the publicly accessible data repository Figshare.

189 **Results**

190 The enhancement effect of SERS is shown in Fig. 1; after the addition of the AgNPs
191 solution in the blood samples, the Raman signal is notably increased as the silver nanostructures
192 are closely adsorbed to the biomolecules present in the plasma (Fig. 1B). The spectral
193 differences between Raman and SERS spectra were expected and can be attributed to the
194 complex nature of the samples, as well as the nonspecific binding of the nanoparticles to the
195 biomolecules.

196 The classification algorithm was performed in both datasets, spontaneous Raman and
197 SERS, to calculate the sensitivity and specificity rates with which these methods can
198 distinguish ovarian cancer patients ($n=27$) and healthy individuals ($n=28$). For the Raman
199 dataset the achieved sensitivity and specificity were 94% and 96%, respectively (Fig. 2A); for
200 the SERS dataset sensitivity and specificity were 87% and 89%, respectively. After the DBM
201 implementation, ten peaks responsible for the differentiation, were selected; out of those, five
202 peaks were picked up by both and Raman and SERS and, therefore, these were used for further
203 statistical analysis (Fig. 3A and 3B). The five peaks that were selected with Raman
204 spectroscopy were: 1657 cm^{-1} (Amide I, $P = 0.0158$; 95% CI = 0.00049 to 0.00471), 1418 cm^{-1}
205 (CH_2 in lipids, $P = 0.0034$; 95% CI = 0.00061 to 0.00334), 1301 cm^{-1} (CH_2 in lipids, $P =$
206 0.0612 ; 95% CI = -0.00379 to 0.00007), 1242 cm^{-1} (Amide III, $P = 0.0103$; 95% CI = -0.00521
207 to -0.00066) and 916 cm^{-1} (amino acids/carbohydrates, $P = 0.0024$; 95% CI = 0.00111 to
208 0.0047), while with SERS: 1655 cm^{-1} (Amide I, $P = 0.0351$; 95% CI = -0.0117 to -0.0005),
209 1429 cm^{-1} (CH_2 in lipids, $P = 0.066$; 95% CI = -0.00049 to 0.00873), 1302 cm^{-1} (CH_2 in lipids,
210 $P = 0.0882$; 95% CI = -0.00825 to 0.00079), 1257 cm^{-1} (Amide III, $P = 0.0003$; 95% CI = -
211 0.00916 to -0.00283) and 919 cm^{-1} (amino acids/carbohydrates, $P = 0.0004$; 95% CI = -0.0067
212 to -0.00163).

213 In order to show that the achieved accuracy was not just due to the difference in the
214 CA-125 levels between cancer patients and healthy individuals, we also performed the SVM
215 classification after taking into account the different protein levels. Sensitivity and specificity
216 remained exceptionally high: Raman yielded 99% sensitivity and 85% specificity after
217 comparing individuals with $\text{CA-125}>35$ (Fig. 4A), as well as 78% sensitivity and 99%
218 specificity for individuals with $\text{CA-125}<35$ (Fig. 4B); SERS achieved sensitivity and
219 specificity of 96% and 74%, respectively, for the group with $\text{CA-125}>35$ (Fig. 4C), as well as
220 72% sensitivity and 97% specificity for the $\text{CA-125}<35$ group (Fig. 4D). Similarly, we

221 considered the age difference between the different groups using the spectra from the
222 spontaneous Raman spectroscopy only (as these provided better results in the previous
223 analyses). The average age of women diagnosed with endometrial cancer is 60 and therefore
224 we considered this as our threshold value. Re-arranging according to age, we had the below
225 cohorts: OC ≥ 60 years ($n=20$), Control ≥ 60 years ($n=10$), OC < 60 years ($n=7$), Control < 60
226 years ($n=19$). After following the same pre-processing and multivariate analysis as previous,
227 we achieved 98% sensitivity and 90% specificity for the older group (≥ 60 years) as well as
228 79% sensitivity and 97% specificity for the younger group (< 60 years) (see SI Fig. S1).

229 Raman and SERS were also used to detect the early ovarian cancer cases ($n=17$) and
230 assess their diagnostic performance. Spontaneous Raman spectroscopy achieved 93%
231 sensitivity and 97% specificity (Fig. 5A), while SERS achieved 80% sensitivity and 94%
232 specificity (Fig. 5B).

233 Discussion

234 Although there has been a great effort in developing biomarkers for the early diagnosis
235 of ovarian cancer, there is still no robust method to achieve this. This study has demonstrated
236 the effectiveness of Raman spectroscopic methods toward the diagnosis of ovarian cancer
237 patients, including early cases. Herein, blood plasma samples were used as a minimally
238 invasive way of specimen collection. Blood biospectroscopy, with either infrared (IR) or
239 Raman, has been previously evaluated in gynecological malignancy. Specifically, IR analysis
240 of plasma and serum was applied to diagnose ovarian and endometrial cancers, providing
241 remarkable accuracy ($\sim 97\%$ for ovarian and $\sim 82\%$ for endometrial cancer) [31]; SERS analysis
242 of plasma achieved 97% sensitivity and 92% specificity for the segregation of cervical cancer
243 cases from normals [32]; cervical cancer and precancer were also detected with serum sample
244 Raman spectroscopy [33]; both IR and spontaneous Raman were used to analyze blood plasma

245 and serum towards the diagnosis of ovarian cancer, yielding 93% accuracy for IR spectra and
246 74% for Raman spectra of plasma [34]; Raman spectroscopy also showed promising results for
247 ovarian cancer diagnosis in 11 patients with the disease, reaching 90% sensitivity and 100%
248 specificity [10]; more recently, it was demonstrated that SERS was able to diagnose
249 endometrial cancer in a pilot study using plasma and serum [35]. Some of the limitations of the
250 above-mentioned studies include either the small number of samples or the absence of a
251 subgroup analysis detecting early stage cases, as well as the lack of CA-125 information as a
252 confounding factor in ovarian cancer. All of these issues have been adequately addressed in
253 the present study. By using a satisfactory number of samples (almost 30 participants in each
254 cohort), we managed to accurately detect both early- and late-stage ovarian cancer cases, which
255 has not been previously shown.

256 In order to overcome the limitation of low signal in spontaneous Raman, SERS using
257 AgNPs was also employed. Another advantage coming with the use of NPs is that they can be
258 used for more specialised analysis if conjugated with targeting biomolecules, such as antibodies
259 [36]. SERS has been shown to substantially increase the Raman signal and be beneficial for
260 single-molecule detection; however, at the same time it presents with a number of limitations,
261 such as lack of reproducibility and preferential metal-molecule binding, which leads to
262 localised enhancement. This may be the reason for the decreased diagnostic accuracy when
263 compared to spontaneous Raman. The preferential enhancement and lack of repeatability in
264 SERS are also reflected by the increased standard deviation in the class means (Fig. 2B).
265 Sensitivities and specificities were substantially high in both SERS (87% and 89%,
266 respectively) and spontaneous Raman (94% and 96%, respectively), with SERS possibly being
267 more sensitive as a biomarker extraction technique.

268 Another plausible explanation for the decreased accuracy in SERS is the use of EDTA
269 during plasma collection. EDTA is a molecule for complexing metal ions and it has been found

270 that its carboxylate groups can bind to nanoparticles surface and be responsible for the
271 generation of new spectral bands [37]. This could potentially obscure the detection of the
272 biological information in the derived spectra. Common anticoagulants used in plasma tubes,
273 such as EDTA and citrate, have been previously found to interfere with SERS spectra; this was
274 suggested to be dealt by the use of serum samples or lithium heparin as the anticoagulant [38].

275 Blood and its constituents are an invaluable source of information, reflecting alterations
276 in the circulation that can be indicative of a change in health status. Recently, circulating
277 tumour DNA (ctDNA) has attracted much attention as a blood biomarker for early and late
278 stage malignancies, introducing an era of “liquid biopsies” [39, 40]. Also, cell-free DNA
279 (cfDNA), reflecting both normal and ctDNA that is released after cellular necrosis and
280 apoptosis, has been previously found significantly increased in the plasma samples of ovarian
281 cancer patients [41]. A recent systematic review and meta-analysis of nine studies (including
282 462 ovarian cancer and 407 controls) concluded that cfDNA diagnosed ovarian cancer with
283 70% sensitivity and 90% specificity and suggested further validation and/or combination with
284 other available biomarkers to improve the diagnostic accuracy [42]. Another study has also
285 shown that ctDNA biomarkers could detect residual tumour, as well as predict response to
286 treatment and survival in ovarian and endometrial cancer cases [43]. With all this in mind, it is
287 quite possible that ctDNA fragments also contributed to the considerably high diagnostic
288 accuracy in this spectroscopic study.

289 Another scope of the current study was to extract spectral biomarkers, responsible for
290 the differentiation between the malignant and healthy individuals. Each spectral peak
291 corresponds to chemical bonds which are present in specific biomolecules; thus, one can
292 tentatively assign a number of disease biomarkers. To achieve this, the difference between
293 ovarian cancer and control spectra was calculated and the ten most discriminating peaks were
294 selected with a peak-detection algorithm; both Raman and SERS revealed five peaks in

295 common and these were chosen for further statistical analysis (Fig. 3). The common peaks
296 were correlated to proteins (Amide I and Amide III), lipids and amino acids/carbohydrates.
297 Surprisingly, two out of five spectral regions ($\sim 1657\text{-}1655\text{ cm}^{-1}$ and $\sim 919\text{-}916\text{ cm}^{-1}$) showed
298 inconsistency between the two spectroscopic approaches; Amide I region was decreased for
299 ovarian cancer patients after Raman spectroscopy, while after SERS the same region was
300 increased. Similarly, the amino acid/carbohydrate region was found decreased in ovarian
301 cancer after Raman and increased after SERS. However, due to the fact that SERS increases
302 significantly the signal of specific peaks, allowing thus more detailed assessment, it is possibly
303 a more sensitive method for biomarker extraction.

304 More than 160 proteins have been reported to be differentially expressed in ovarian
305 cancer, with some being upregulated, such as CA-125, CA19-9, HE4 or mesothelin, and other
306 being downregulated, such as epidermal growth factor receptor (EGFR) and ApoA1 [44].
307 Amide I ($\sim 1650\text{ cm}^{-1}$) and Amide III ($\sim 1300\text{ cm}^{-1}$) bands represent protein molecules and are
308 mainly associated with the C=O stretching and C-N stretching/N-H bending vibrations,
309 respectively. The increased level of Amide I and Amide III in ovarian cancer patients after
310 SERS, may correlate with the changes occurring due to the overexpressed proteins. The
311 spectral bands indicative of lipids were both decreased (1429 cm^{-1}) and increased (1302 cm^{-1})
312 in the ovarian cancer group, which is also backed by previous studies showing a dysregulation
313 of lipid metabolism in cancer [45]. For instance, some studies have shown increased lipid levels
314 in ovarian cancer [45-47], while a limited number of studies have reported reduction [47, 48].
315 An alternative interpretation of the decreased lipid region (1429 cm^{-1}) could be the
316 downregulation of ApoA1 which has been previously shown to diagnose ovarian cancer in
317 plasma and was estimated at $1484\text{-}1427\text{ cm}^{-1}$ [49]. The rise seen in the amino
318 acids/carbohydrate region (919 cm^{-1}) could potentially be attributed to ctDNA, as discussed

319 previously, or correlated with increased amount of carbohydrates which is considered a risk
320 factor for ovarian cancer [50, 51].

321 Previous spectroscopic studies investigating ovarian malignancy have not taken into account
322 the differences between CA-125 levels, which may have led to an unrealistic segregation
323 between patients and healthy controls. In order to investigate whether the high diagnostic
324 accuracies achieved in our study were actually attributed to the presence of cancer or just the
325 difference in the CA-125 levels, we also carried out a subgroup analysis to account for this.
326 The extra analysis showed that sensitivities and specificities remained equally satisfactory
327 which denotes that the differences found in our cohort were not attributed to CA-125 but rather
328 to the cancerous condition. Also, after accounting for age differences, it was evident that age
329 alone was not the reason for the high diagnostic accuracy. Even though there is a slight decrease
330 in sensitivity and specificity (*i.e.*, for ≥ 60 years, specificity dropped from 96% to 90%; for < 60
331 years, sensitivity dropped from 94% to 79%), the diagnostic capability remained very high.

332 Improved diagnostic performance for the early-stage ovarian cases was a critical
333 objective of this study in order to allow early intervention and potentially improve patient
334 outcomes. Again, both spectroscopic methods provided outstanding diagnostic accuracy, with
335 Raman (sensitivity: 93% and specificity: 97%) being superior to SERS (sensitivity: 80% and
336 specificity: 94%). Current approaches for the early detection of ovarian cancer include
337 biomarker tests, such as serum CA-125 and HE4, imaging techniques, such as computed
338 tomography (CT), transvaginal ultrasound (TVUS) and positron emission tomography (PET)
339 or a combination of these [52]. However, there are still a number of limitations in these methods
340 including expense and lack of optimal sensitivity and specificity. For instance, the sensitivity
341 and specificity of CA-125 is known to be poor, with only 50% of the patients having elevated
342 levels of the protein at stage I and ~75-90% of the cases at a later stage [4]. CA-125 level can
343 be used more reliably to monitor treatment as levels of CA-125 decrease when a treatment is

344 efficient. However, it is not useful for screening as CA-125 level can be elevated in other
345 conditions, such as endometriosis, breast or lung malignancies, and also not every woman with
346 ovarian cancer has elevated CA-125; CT is expensive and has high false-positive rates which
347 prevent its use in screening [1]. Even though TVUS is preferred than other imaging techniques
348 in terms of speed and sensitivity, there is yet no convincing evidence that it detects early
349 ovarian cancer without causing overtreatment of non-malignant cases [2]. TVUS can indeed
350 show a mass in the ovary but it cannot distinguish whether the mass is benign or malignant.
351 Therefore, other blood biomarkers (CA-125) are used together with ultrasound to identify
352 ovarian tumour at high risk of malignancy. Previous large cohort studies have evaluated the
353 sensitivity and specificity of multimodal screening (MMS) (i.e., annual testing of CA-125 with
354 ultrasound scan as a second line test) and ultrasound screening (USS) (i.e., ultrasound alone);
355 their results showed that the MMS gave slightly higher sensitivity [5, 53]. Specifically, the
356 overall sensitivity for detection of ovarian cancers, diagnosed within a year of a screening, was
357 84% in the MMS group and 73% in the USS group [5]. However, the positive predictive value
358 for USS was estimated at around ~5%, which indicates a quite high false-positive rate [53]. In
359 an effort to improve the diagnostic accuracy many groups have also combined different
360 biomarkers, which however increase the cost and time requirement [1, 44]. By using
361 spectroscopic techniques these drawbacks seem to be eliminated as they provide a simpler,
362 cost-effective, multi-marker assay, thus securing robustness. The diagnostic accuracy shown
363 in this study is even better than the currently used tests.

364 In conclusion, the efficacy of Raman spectroscopic methods (i.e., spontaneous Raman
365 and SERS) in detecting ovarian cancer, including early-stage patients, has been demonstrated.
366 Continuous efforts are being made to improve clinical diagnosis and monitoring of disease in
367 ovarian cancer. Our findings suggest improved diagnostic accuracy compared to traditional
368 biomarkers. Specific biomolecules were also found responsible for the segregation between the

369 cancer and healthy cases and could be used as spectral biomarkers. Future spectroscopic studies
370 should focus on the validation of these results in larger datasets and across different scientific
371 groups and laboratories; this would open a new road in ovarian cancer research and potentially
372 allow the implementation of blood spectroscopy in clinical practice as a promising diagnostic
373 tool.

374 [Acknowledgements](#)

375 MP acknowledges Rosemere Cancer Foundation for funding. Special thanks to Emma Callery
376 and Debra Beesley for conducting the serum CA-125 tests.

377 [Availability of data and materials](#)

378 All raw and pre-processed spectra will be available at the publicly accessible data repository
379 Figshare.

380 [Disclosure/Conflict of Interest](#)

381 The authors declare no conflicts of interest

382 [Authorship](#)

383 FLM and PLMH conceived the study; MP designed the study, conducted the spectroscopic,
384 multivariate/statistical analysis and wrote the manuscript; KA, HFS, NW, PK, AR and PLMH
385 collected and provided the samples. All authors provided constructive feedback during
386 manuscript preparation. All authors have approved the final version.

387

388 [References](#)

- 389 [1] Z. Yurkovetsky, S. Skates, A. Lomakin, B. Nolen, T. Pulsipher, F. Modugno, J. Marks, A. Godwin, E.
390 Gorelik, I. Jacobs, Development of a multimarker assay for early detection of ovarian cancer, *J Clin*
391 *Oncol* 28(13) (2010) 2159-2166.
392 [2] G.C. Jayson, E.C. Kohn, H.C. Kitchener, J.A. Ledermann, Ovarian cancer, *Lancet* 384(9951) (2014)
393 1376-1388.
394 [3] C.H. Holschneider, J.S. Berek, Ovarian cancer: epidemiology, biology, and prognostic factors,
395 *Semin Surg Oncol*, Wiley Online Library, 2000, pp. 3-10.
396 [4] E. Moss, J. Hollingworth, T. Reynolds, The role of CA125 in clinical practice, *J. Clin. Pathol.* 58(3)
397 (2005) 308-312.
398 [5] I.J. Jacobs, U. Menon, A. Ryan, A. Gentry-Maharaj, M. Burnell, J.K. Kalsi, N.N. Amso, S.
399 Apostolidou, E. Benjamin, D. Cruickshank, Ovarian cancer screening and mortality in the UK
400 Collaborative Trial of Ovarian Cancer Screening (UKCTOCS): a randomised controlled trial, *Lancet*
401 387(10022) (2016) 945-956.

402 [6] E. Kobayashi, Y. Ueda, S. Matsuzaki, T. Yokoyama, T. Kimura, K. Yoshino, M. Fujita, T. Kimura, T.
403 Enomoto, Biomarkers for screening, diagnosis, and monitoring of ovarian cancer, *Cancer Epidemiol*
404 *Biomarkers Prevent* 21(11) (2012) 1902-1912.

405 [7] F. Su, J. Lang, A. Kumar, C. Ng, B. Hsieh, M.A. Suchard, S.T. Reddy, R. Farias-Eisner, Validation of
406 candidate serum ovarian cancer biomarkers for early detection, *Biomark Insights* 2 (2007) 369.

407 [8] V. Nossov, M. Amneus, F. Su, J. Lang, J.M.T. Janco, S.T. Reddy, R. Farias-Eisner, The early
408 detection of ovarian cancer: from traditional methods to proteomics. Can we really do better than
409 serum CA-125?, *Am J Obstet Gynecol* 199(3) (2008) 215-223.

410 [9] I. Visintin, Z. Feng, G. Longton, D.C. Ward, A.B. Alvero, Y. Lai, J. Tenthorey, A. Leiser, R. Flores-
411 Saaib, H. Yu, Diagnostic markers for early detection of ovarian cancer, *Clin Cancer Res* 14(4) (2008)
412 1065-1072.

413 [10] I. Ullah, I. Ahmad, H. Nisar, S. Khan, R. Ullah, R. Rashid, H. Mahmood, Computer assisted optical
414 screening of human ovarian cancer using Raman spectroscopy, *Photodiagnosis Photodyn Ther* 15
415 (2016) 94-99.

416 [11] I. Pence, A. Mahadevan-Jansen, Clinical instrumentation and applications of Raman
417 spectroscopy, *Chem Soc Rev* 45(7) (2016) 1958-1979.

418 [12] I.P. Santos, E.M. Barroso, T.C. Bakker Schut, P.J. Caspers, C.G.F. van Lanschot, D.H. Choi, M.F.
419 van der Kamp, R.W.H. Smits, R. van Doorn, R.M. Verdijk, V. Noordhoek Hegt, J.H. von der Thusen,
420 C.H.M. van Deurzen, L.B. Koppert, G. van Leenders, P.C. Ewing-Graham, H.C. van Doorn, C.M.F.
421 Dirven, M.B. Busstra, J. Hardillo, A. Sewnaik, I. Ten Hove, H. Mast, D.A. Monserez, C. Meeuwis, T.
422 Nijsten, E.B. Wolvius, R.J. Baatenburg de Jong, G.J. Puppels, S. Koljenovic, Raman spectroscopy for
423 cancer detection and cancer surgery guidance: translation to the clinics, *Analyst* 142 (2017) 3025-47.

424 [13] F.L. Cals, T.C. Bakker Schut, J.A. Hardillo, R.J. Baatenburg de Jong, S. Koljenovic, G.J. Puppels,
425 Investigation of the potential of Raman spectroscopy for oral cancer detection in surgical margins,
426 *Lab Invest* 95(10) (2015) 1186-96.

427 [14] M.D. Keller, E. Vargis, N. de Matos Granja, R.H. Wilson, M.A. Mycek, M.C. Kelley, A. Mahadevan-
428 Jansen, Development of a spatially offset Raman spectroscopy probe for breast tumor surgical
429 margin evaluation, *J Biomed Opt* 16(7) (2011) 077006.

430 [15] K. Kong, C. Kendall, N. Stone, I. Notingher, Raman spectroscopy for medical diagnostics — From
431 in-vitro biofluid assays to in-vivo cancer detection, *Adv Drug Del Rev* 89 (2015) 121-134.

432 [16] M. Jermyn, K. Mok, J. Mercier, J. Desroches, J. Pichette, K. Saint-Arnaud, L. Bernstein, M.C.
433 Guiot, K. Petrecca, F. Leblond, Intraoperative brain cancer detection with Raman spectroscopy in
434 humans, *Sci Transl Med* 7(274) (2015) 274ra19.

435 [17] F.M. Lyng, D. Traynor, I.R. Ramos, F. Bonnier, H.J. Byrne, Raman spectroscopy for screening and
436 diagnosis of cervical cancer, *Anal Bioanal Chem* 407(27) (2015) 8279-89.

437 [18] M. Paraskevaidi, C.L. Morais, D.E. Halliwell, D.M. Mann, D. Allsop, P.L. Martin-Hirsch, F.L. Martin,
438 Raman spectroscopy to diagnose Alzheimer's disease and dementia with Lewy bodies in blood, *ACS*
439 *Chem Neurosci* (2018).

440 [19] M. Paraskevaidi, C. de Morais, K.M.G. de Lima, K. Ashton, H.F. Stringfellow, P.L. Martin-Hirsch,
441 F.L. Martin, Potential of mid-infrared spectroscopy as a non-invasive diagnostic test in urine for
442 endometrial or ovarian cancer, *Analyst* (2018).

443 [20] C.M. Krishna, G. Sockalingum, L. Venteo, R.A. Bhat, P. Kushtagi, M. Pluot, M. Manfait, Evaluation
444 of the suitability of ex vivo handled ovarian tissues for optical diagnosis by Raman
445 microspectroscopy, *Biopolymers* 79(5) (2005) 269-276.

446 [21] R. Mehrotra, G. Tyagi, D.K. Jangir, R. Dawar, N. Gupta, Analysis of ovarian tumor pathology by
447 Fourier Transform Infrared Spectroscopy, *J Ovarian Res* 3(1) (2010) 27.

448 [22] G. Theophilou, K.M.G. Lima, P.L. Martin-Hirsch, H.F. Stringfellow, F.L. Martin, ATR-FTIR
449 spectroscopy coupled with chemometric analysis discriminates normal, borderline and malignant
450 ovarian tissue: classifying subtypes of human cancer, *Analyst* 141(2) (2016) 585-594.

451 [23] A.L. Mitchell, K.B. Gajjar, G. Theophilou, F.L. Martin, P.L. Martin-Hirsch, Vibrational spectroscopy
452 of biofluids for disease screening or diagnosis: translation from the laboratory to a clinical setting, *J*
453 *Biophotonics* 7(3-4) (2014) 153-165.

454 [24] M. Paraskevaïdi, C.L. Morais, K.M. Lima, J.S. Snowden, J.A. Saxon, A.M. Richardson, M. Jones,
455 D.M. Mann, D. Allsop, P.L. Martin-Hirsch, Differential diagnosis of Alzheimer's disease using
456 spectrochemical analysis of blood, *Proc Natl Acad Sci USA* (2017) 201701517.

457 [25] N. MacRitchie, G. Grassia, J. Noonan, P. Garside, D. Graham, P. Maffia, Molecular imaging of
458 atherosclerosis: spotlight on Raman spectroscopy and surface-enhanced Raman scattering, *Heart*
459 (2017) heartjnl-2017-311447.

460 [26] B. Fazio, C. D'Andrea, A. Foti, E. Messina, A. Irrera, M.G. Donato, V. Villari, N. Micali, O.M.
461 Maragò, P.G. Gucciardi, SERS detection of Biomolecules at Physiological pH via aggregation of Gold
462 Nanorods mediated by Optical Forces and Plasmonic Heating, *Sci Rep* 6 (2016) 26952.

463 [27] H.J. Butler, L. Ashton, B. Bird, G. Cinque, K. Curtis, J. Dorney, K. Esmonde-White, N.J. Fullwood,
464 B. Gardner, P.L. Martin-Hirsch, M.J. Walsh, M.R. McAinsh, N. Stone, F.L. Martin, Using Raman
465 spectroscopy to characterize biological materials, *Nat Protoc* 11(4) (2016) 664-687.

466 [28] M.J. Baker, J. Trevisan, P. Bassan, R. Bhargava, H.J. Butler, K.M. Dorling, P.R. Fielden, S.W.
467 Fogarty, N.J. Fullwood, K.A. Heys, C. Hughes, P. Lasch, P.L. Martin-Hirsch, B. Obinaju, G.D.
468 Sockalingum, J. Sulé-Suso, R.J. Strong, M.J. Walsh, B.R. Wood, P. Gardner, F.L. Martin, Using Fourier
469 transform IR spectroscopy to analyze biological materials, *Nat Protoc* 9(8) (2014) 1771-1791.

470 [29] C.-W. Hsu, C.-C. Chang, C.-J. Lin, A practical guide to support vector classification, (2003),
471 ([https://www.researchgate.net/profile/Chenghai_Yang/publication/272039161_Evaluating_unsuper
472 vised_and_supervised_image_classification_methods_for_mapping_cotton_root_rot/links/55f2c574
473 08ae0960a3897985/Evaluating-unsupervised-and-supervised-image-classification-methods-for-
474 mapping-cotton-root-rot.pdf](https://www.researchgate.net/profile/Chenghai_Yang/publication/272039161_Evaluating_unsuper_vised_and_supervised_image_classification_methods_for_mapping_cotton_root_rot/links/55f2c574_08ae0960a3897985/Evaluating-unsupervised-and-supervised-image-classification-methods-for-mapping-cotton-root-rot.pdf)).

475 [30] J. Trevisan, P.P. Angelov, P.L. Carmichael, A.D. Scott, F.L. Martin, Extracting biological
476 information with computational analysis of Fourier-transform infrared (FTIR) biospectroscopy
477 datasets: current practices to future perspectives, *Analyst* 137(14) (2012) 3202-15.

478 [31] K. Gajjar, J. Trevisan, G. Owens, P.J. Keating, N.J. Wood, H.F. Stringfellow, P.L. Martin-Hirsch, F.L.
479 Martin, Fourier-transform infrared spectroscopy coupled with a classification machine for the
480 analysis of blood plasma or serum: a novel diagnostic approach for ovarian cancer, *Analyst* 138(14)
481 (2013) 3917-26.

482 [32] S. Feng, D. Lin, J. Lin, B. Li, Z. Huang, G. Chen, W. Zhang, L. Wang, J. Pan, R. Chen, Blood plasma
483 surface-enhanced Raman spectroscopy for non-invasive optical detection of cervical cancer, *Analyst*
484 138(14) (2013) 3967-3974.

485 [33] J.L. González-Solís, J.C. Martínez-Espinosa, L.A. Torres-González, A. Aguilar-Lemarroy, L.F. Jave-
486 Suárez, P. Palomares-Anda, Cervical cancer detection based on serum sample Raman spectroscopy,
487 *Lasers Med Sci* 29(3) (2014) 979-985.

488 [34] G.L. Owens, K. Gajjar, J. Trevisan, S.W. Fogarty, S.E. Taylor, B. Da Gama-Rose, P.L. Martin-Hirsch,
489 F.L. Martin, Vibrational biospectroscopy coupled with multivariate analysis extracts potentially
490 diagnostic features in blood plasma/serum of ovarian cancer patients, *J Biophotonics* 7(3-4) (2014)
491 200-9.

492 [35] H.J. Butler, S.W. Fogarty, J.G. Kerns, P.L. Martin-Hirsch, N.J. Fullwood, F.L. Martin, Gold
493 nanoparticles as a substrate in bio-analytical near-infrared surface-enhanced Raman spectroscopy,
494 *Analyst* 140(9) (2015) 3090-3097.

495 [36] M. Arruebo, M. Valladares, Á. González-Fernández, Antibody-conjugated nanoparticles for
496 biomedical applications, *J Nanomater* 2009 (2009) 37.

497 [37] S. Mondal, S. Verma, Catalytic and SERS Activities of Tryptophan-EDTA Capped Silver
498 Nanoparticles, *Z Anorg Allg Chem* 640(6) (2014) 1095-1101.

499 [38] A. Bonifacio, S. Dalla Marta, R. Spizzo, S. Cervo, A. Steffan, A. Colombatti, V. Sergo, Surface-
500 enhanced Raman spectroscopy of blood plasma and serum using Ag and Au nanoparticles: a
501 systematic study, *Anal Bioanal Chem* 406(9-10) (2014) 2355-2365.

502 [39] C. Bettegowda, M. Sausen, R.J. Leary, I. Kinde, Y. Wang, N. Agrawal, B.R. Bartlett, H. Wang, B.
503 Luber, R.M. Alani, Detection of circulating tumor DNA in early-and late-stage human malignancies,
504 *Sci Transl Med* 6(224) (2014) 224ra24-224ra24.

505 [40] L.A. Diaz Jr, A. Bardelli, Liquid biopsies: genotyping circulating tumor DNA, *J Clin Oncol* 32(6)
506 (2014) 579-586.

507 [41] A.A. Kamat, M. Baldwin, D. Urbauer, D. Dang, L.Y. Han, A. Godwin, B.Y. Karlan, J.L. Simpson,
508 D.M. Gershenson, R.L. Coleman, Plasma cell-free DNA in ovarian cancer, *Cancer* 116(8) (2010) 1918-
509 1925.

510 [42] Q. Zhou, W. Li, B. Leng, W. Zheng, Z. He, M. Zuo, A. Chen, Circulating cell free DNA as the
511 diagnostic marker for ovarian cancer: A systematic review and meta-analysis, *PloS one* 11(6) (2016)
512 e0155495.

513 [43] E. Pereira, O. Camacho-Vanegas, S. Anand, R. Sebra, S.C. Camacho, L. Garnar-Wortzel, N. Nair, E.
514 Moshier, M. Wooten, A. Uzilov, Personalized circulating tumor DNA biomarkers dynamically predict
515 treatment response and survival in gynecologic cancers, *PLoS One* 10(12) (2015) e0145754.

516 [44] B.M. Nolen, A.E. Lokshin, Protein biomarkers of ovarian cancer: the forest and the trees, *Future*
517 *Oncol* 8(1) (2012) 55-71.

518 [45] C.R. Santos, A. Schulze, Lipid metabolism in cancer, *FEBS J.* 279(15) (2012) 2610-2623.

519 [46] I. Delimaris, E. Faviou, G. Antonakos, E. Stathopoulou, A. Zachari, A. Dionyssiou-Asteriou,
520 Oxidized LDL, serum oxidizability and serum lipid levels in patients with breast or ovarian cancer, *Clin*
521 *Biochem* 40(15) (2007) 1129-1134.

522 [47] M. Tania, M. Khan, Y. Song, Association of lipid metabolism with ovarian cancer, *Curr Oncol*
523 17(5) (2010) 6.

524 [48] Q. Hu, M. Wang, M.S. Cho, C. Wang, A.M. Nick, P. Thiagarajan, F.M. Aung, X. Han, A.K. Sood, V.
525 Afshar-Kharghan, Lipid profile of platelets and platelet-derived microparticles in ovarian cancer, *BBA*
526 *clinical* 6 (2016) 76-81.

527 [49] G. Deleris, C. Petibois, Applications of FT-IR spectrometry to plasma contents analysis and
528 monitoring, *Vib Spectrosc* 32(1) (2003) 129-136.

529 [50] L. Augustin, J. Polesel, C. Bosetti, C. Kendall, C. La Vecchia, M. Parpinel, E. Conti, M. Montella, S.
530 Franceschi, D. Jenkins, Dietary glycemic index, glycemic load and ovarian cancer risk: a case-control
531 study in Italy, *Ann Oncol* 14(1) (2003) 78-84.

532 [51] B. Qin, P.G. Moorman, A.J. Alberg, J.S. Barnholtz-Sloan, M. Bondy, M.L. Cote, E. Funkhouser, E.S.
533 Peters, A.G. Schwartz, P. Terry, Dietary carbohydrate intake, glycaemic load, glycaemic index and
534 ovarian cancer risk in African-American women, *Br J Nutr* 115(4) (2016) 694-702.

535 [52] J.V. Jokerst, A.J. Cole, D. Van de Sompel, S.S. Gambhir, Gold nanorods for ovarian cancer
536 detection with photoacoustic imaging and resection guidance via Raman imaging in living mice, *ACS*
537 *Nano* 6(11) (2012) 10366-10377.

538 [53] U. Menon, A. Gentry-Maharaj, R. Hallett, A. Ryan, M. Burnell, A. Sharma, S. Lewis, S. Davies, S.
539 Philpott, A. Lopes, Sensitivity and specificity of multimodal and ultrasound screening for ovarian
540 cancer, and stage distribution of detected cancers: results of the prevalence screen of the UK
541 Collaborative Trial of Ovarian Cancer Screening (UKCTOCS), *Lancet Oncol* 10(4) (2009) 327-340.

542 [54] Z. Movasaghi, S. Rehman, I.U. Rehman, Raman spectroscopy of biological tissues, *Appl Spectrosc*
543 *Rev* 42(5) (2007) 493-541.

544 [55] S. Li, L. Li, Q. Zeng, Y. Zhang, Z. Guo, Z. Liu, M. Jin, C. Su, L. Lin, J. Xu, S. Liu, Characterization and
545 noninvasive diagnosis of bladder cancer with serum surface enhanced Raman spectroscopy and
546 genetic algorithms, *Sci Rep* 5 (2015) 9582.

547 [56] D. Lin, S. Feng, J. Pan, Y. Chen, J. Lin, G. Chen, S. Xie, H. Zeng, R. Chen, Colorectal cancer
548 detection by gold nanoparticle based surface-enhanced Raman spectroscopy of blood serum and
549 statistical analysis, *Opt Express* 19(14) (2011) 13565-13577.

550 [57] S. Feng, R. Chen, J. Lin, J. Pan, G. Chen, Y. Li, M. Cheng, Z. Huang, J. Chen, H. Zeng,
551 Nasopharyngeal cancer detection based on blood plasma surface-enhanced Raman spectroscopy
552 and multivariate analysis, *Biosens Bioelectron* 25(11) (2010) 2414-2419.

553 [58] J.L. Pichardo-Molina, C. Frausto-Reyes, O. Barbosa-García, R. Huerta-Franco, J.L. González-
554 Trujillo, C.A. Ramírez-Alvarado, G. Gutiérrez-Juárez, C. Medina-Gutiérrez, Raman spectroscopy and
555 multivariate analysis of serum samples from breast cancer patients, *Lasers Med Sci* 22(4) (2007) 229-
556 236.

557

558

559

560

561

562

563

564

565

566

567

568

569

570

571

572

573

574

575

576

577

578

579

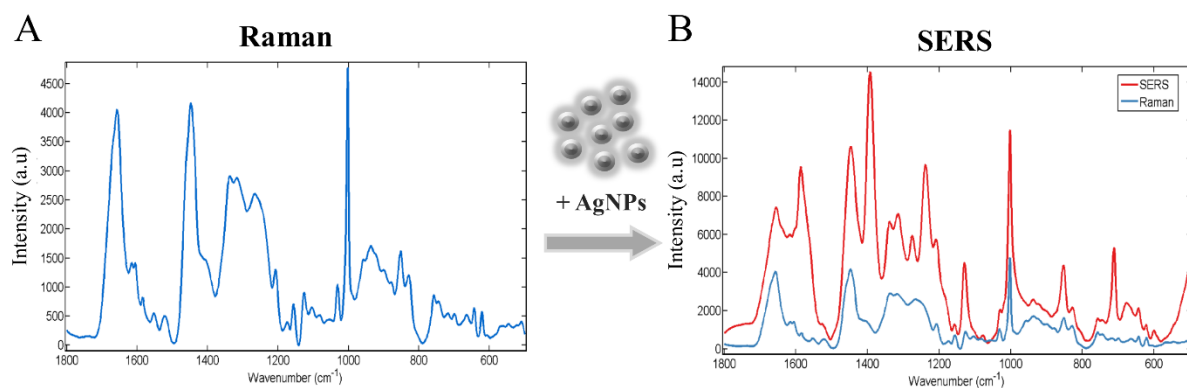
580

581

582

583

584 Figure Legends



585

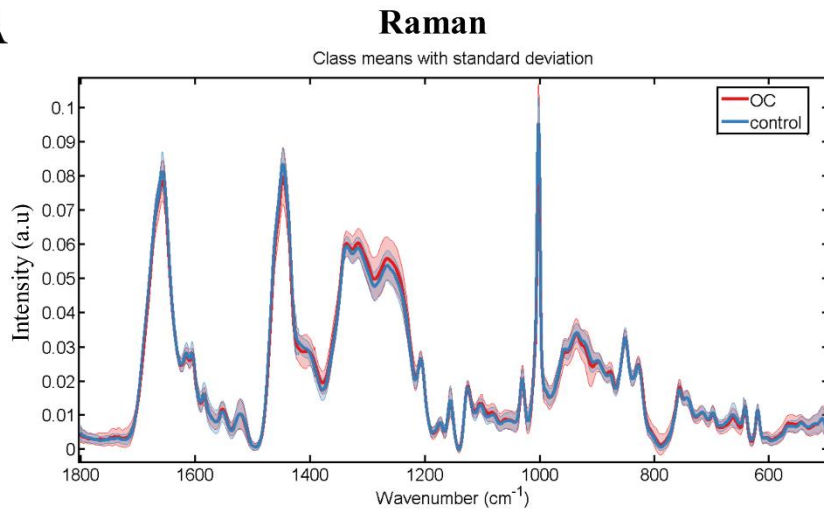
586 **Figure 1:** Enhancement effect of SERS after the addition of silver nanoparticles (AgNPs) in
587 blood samples.

588

589

590

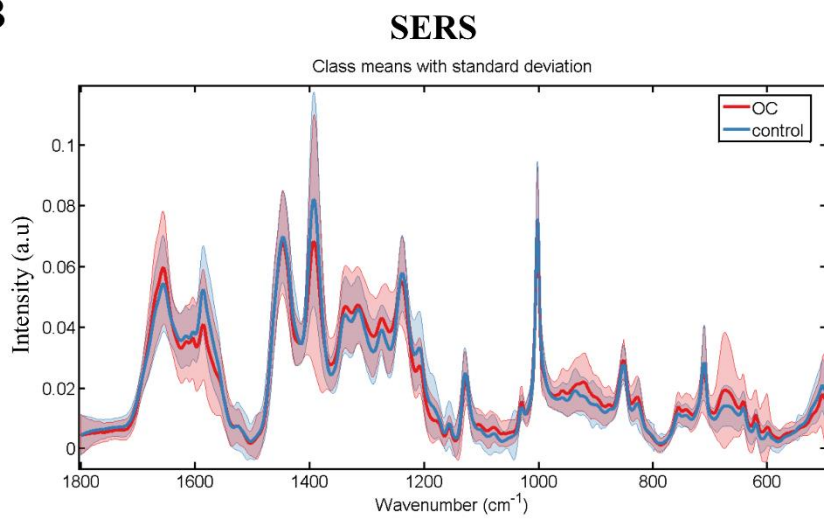
A



Sensitivity: 94%

Specificity: 96%

B

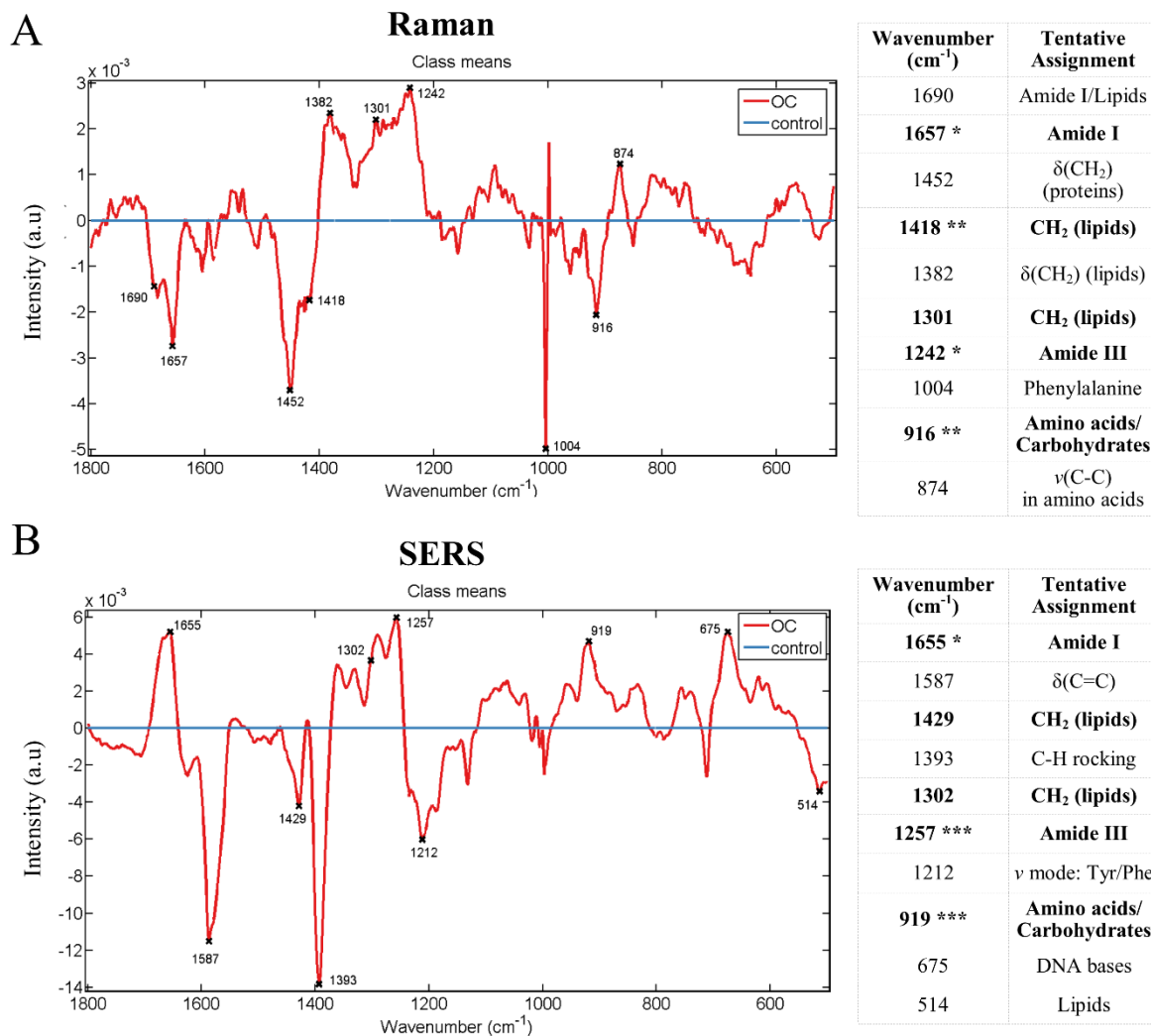


Sensitivity: 87%

Specificity: 89%

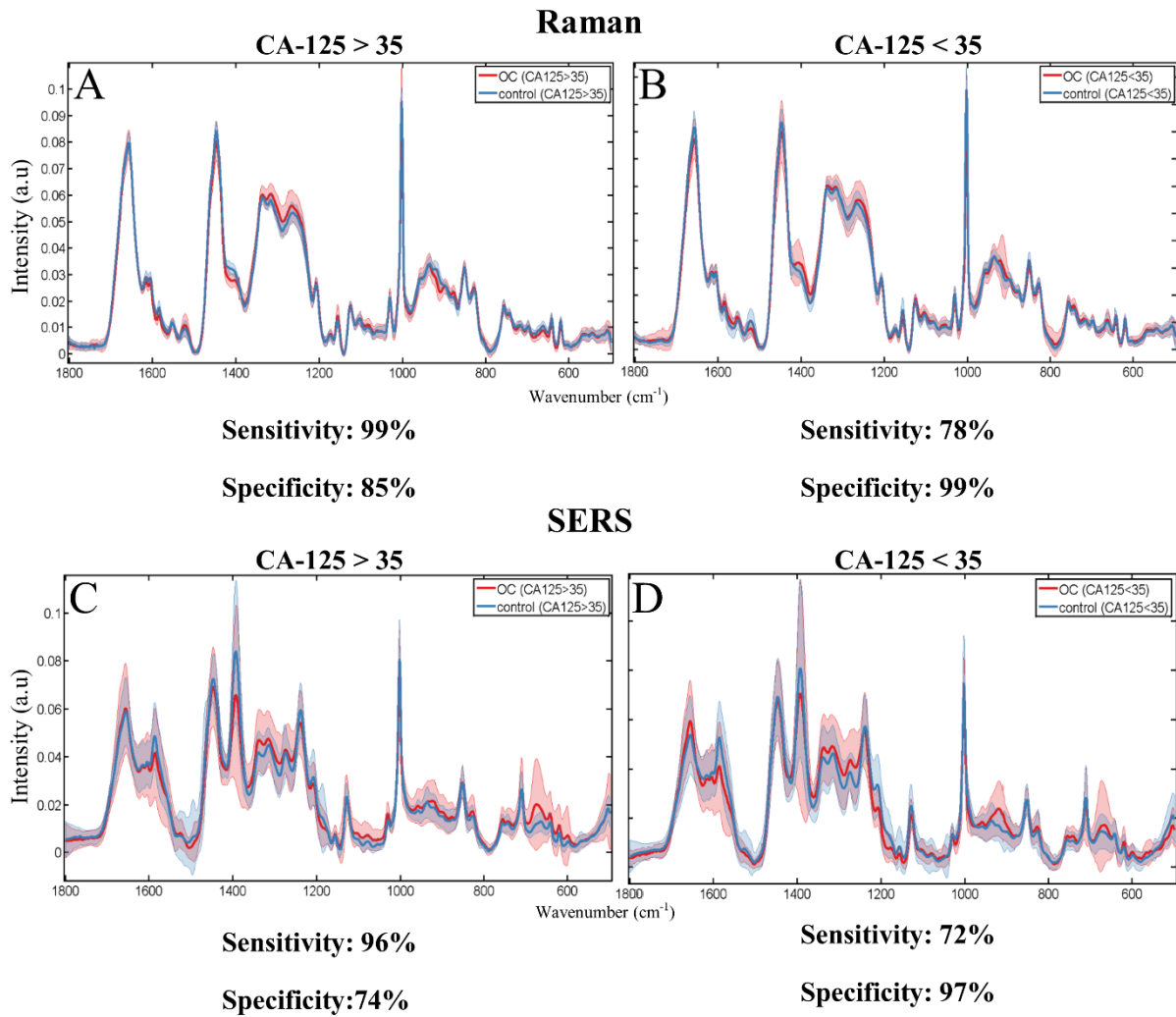
591

592 **Figure 2:** Diagnostic segregation of ovarian cancer (OC) with (A) Raman spectroscopy and
593 (B) SERS.



594

595 **Figure 3:** Differentiating spectral peaks after (A) Raman spectroscopy and (B) SERS. The
 596 tables show the peak positions and tentative assignments of major vibrational bands [54-58];
 597 peaks shown with bold were detected with both Raman and SERS and may be used as more
 598 reliable diagnostic biomarkers. Abbreviations: OC: ovarian cancer; ν : stretching mode; δ :
 599 bending mode.

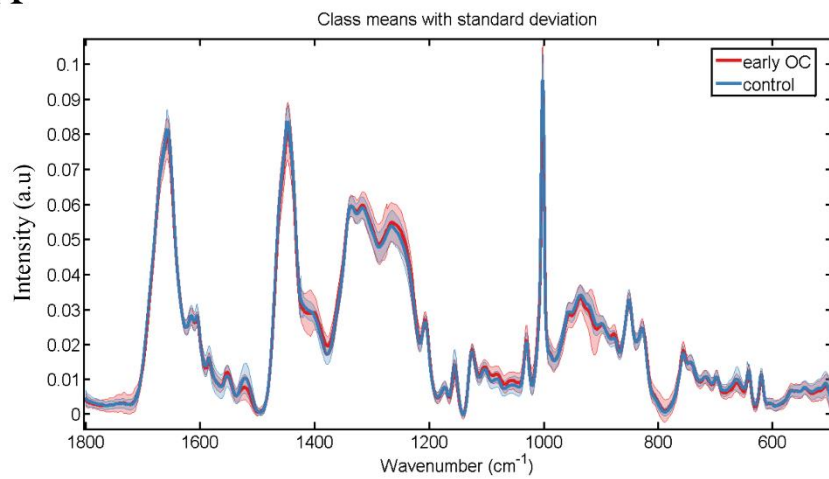


600

601 **Figure 4:** Diagnostic segregation between ovarian cancer (OC) patients and healthy controls
 602 according to their CA-125 levels. Sensitivity and specificity are provided for (A) individuals
 603 with CA-125>35 u/ml after Raman analysis, (B) individuals with CA-125<35 u/ml after
 604 Raman, (C) individuals with CA-125>35 u/ml after SERS and (D) individuals with CA-125<35
 605 u/ml after SERS.

A

Raman

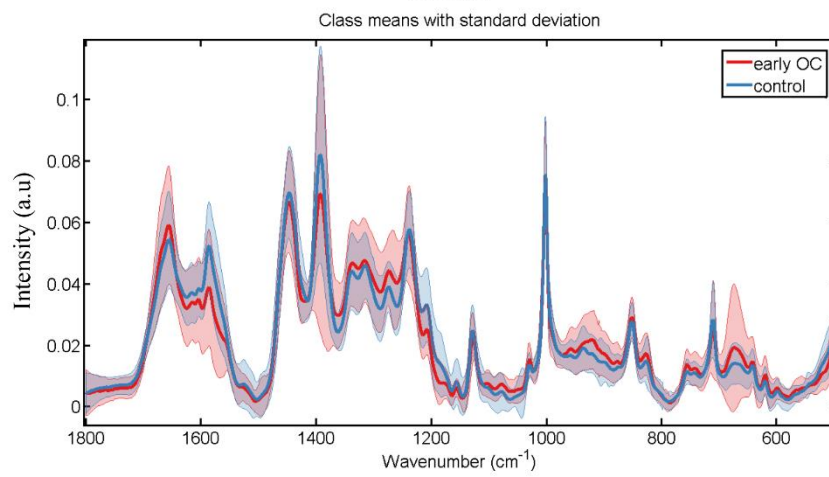


Sensitivity: 93%

Specificity: 97%

B

SERS



Sensitivity: 80%

Specificity: 94%

606

607 **Figure 5:** Diagnosis of early ovarian cancer (OC) after (A) Raman spectroscopy and (B) SERS.